Environmental Science & Technology

Article

pubs.acs.org/est

Production of Molecular Iodine and Tri-iodide in the Frozen Solution of Iodide: Implication for Polar Atmosphere

Kitae Kim,[†,‡] Akihiro Yabushita,[§,∥] Masanori Okumura,[§] Alfonso Saiz-Lopez,[⊥] Carlos A. Cuevas,[⊥] Christopher S. Blaszczak-Boxe,[#] Dae Wi Min,[†] Ho-Il Yoon,[‡] and Wonyong Choi*[,†]

[†]School of Environmental Science and Engineering, Pohang University of Science and Technology (POSTECH), Pohang 790-784, Korea

[‡]Korea Polar Research Institute (KOPRI), Incheon 406-840, Korea

[§]Department of Molecular Engineering, Kyoto University, Kyoto 615-8510, Japan

[∥]Department of Molecular and Material Sciences, Kyushu University, Kasuga, Fukuoka 816-8580, Japan

[⊥]Department of Atmospheric Chemistry and Climate, Institute of Physical Chemistry Rocasolano, CSIC, Madrid, Spain

[#]Department of Physical, Environmental and Computer Sciences Medgar Evers College-City, University of New York, Brooklyn, New York 11235, United States

Supporting Information

ABSTRACT: The chemistry of reactive halogens in the polar atmosphere plays important roles in ozone and mercury depletion events, oxidizing capacity, and dimethylsulfide oxidation to form cloud-condensation nuclei. Among halogen species, the sources and emission mechanisms of inorganic iodine compounds in the polar boundary layer remain unknown. Here, we demonstrate that the production of tri-iodide (I_3^-) via iodide oxidation, which is negligible in aqueous solution, is significantly accelerated in frozen solution, both in the presence and the absence of solar irradiation. Field experiments carried out in the Antarctic region (King George Island, 62°13′S, 58°47′W) also showed that the generation of tri-iodide via solar photo-oxidation was enhanced when iodide was added to various ice media. The emission of gaseous I_2 from the irradiated frozen solution of iodide to the gas phase was detected by using cavity ring-down spectroscopy, which was observed both in the frozen state at 253 K and after thawing the ice at 298 K. The accelerated (photo-)oxidation of iodide and the subsequent formation of tri-iodide and I_2 in ice appear to be related with the freeze concentration of iodide and dissolved O_2 trapped in the ice crystal grain boundaries. We propose that an accelerated abiotic transformation of iodide to gaseous I_2 in ice media provides a previously unrecognized formation pathway of active iodine species in the polar atmosphere.

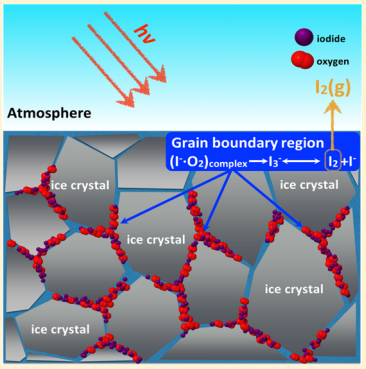

INTRODUCTION

Reactive halogens play various key roles in the global environment. In particular, the presence of gaseous halogens in the polar and marine boundary layers is of great interest because these highly reactive species can affect the oxidative capacity of Earth's atmosphere.[1−9] The sources and impacts of iodine in polar atmospheric chemistry are much less understood in comparison with chlorine and bromine. Although active iodine compounds (e.g., IO and I_2) in the polar regions have been observed by ground- and satellite-based techniques, the sources and mechanisms of this large iodine emission are still being debated.[4−6,10,11] In this aspect, it is of particular interest how the heterogeneous chemistry of iodine can be affected by the presence of frozen media in cold environments such as the polar region. Some chemical and photochemical reactions in frozen solutions are reported to be quite different from their aqueous counterparts and highly accelerated because solutes are concentrated in liquid-like grain boundary regions (freeze concentration effect)[12−20] and brine channels in sea ice[21,22] as they are segregated from the crystalline ice lattice.

A number of atmospherically relevant oxidation reactions, such as nitrite to nitrate and sulfite or sulfide to sulfate, are known to be promoted when dilute solutions are frozen.[12,23,24] O'Driscoll et al.[23] reported that the enhanced release of active and ozone-depleting gases such as nitric oxide (NO) and iodine molecule (I_2) from the solidification of sea-salt aerosol components containing nitrite and iodide ion (NO_2^-/I^-). They observed the production of I_3^- spectrophotometrically in the frozen solution of $NaNO_2$/KI at pH 6. Sullivan and Sodeau[25] investigated the freeze-induced formation of interhalogen species from frozen halide ion solutions that can be a potential mechanism for the release of interhalogens to the atmosphere in polar regions. In this study, they observed the freeze-induced production of dibromoiodide ion, IBr_2^- from mixed solutions containing iodide, bromide, and nitrite ions

Received: October 20, 2015
Revised: January 6, 2016
Accepted: January 8, 2016
Published: January 8, 2016

DOI: 10.1021/acs.est.5b05148
Environ. Sci. Technol. 2016, 50, 1280−1287

under slightly acidic conditions up to pH 5.1, which is relevant to snow in polar region. They also verified the effects of various experimental conditions such as a ratio of $[Br^-]/[I^-]$, pH, and the presence of oxidants (nitrite and hydrogen peroxide) and dioxygen. Diao and Chu also investigated the heterogeneous reactions of gaseous HONO with HCl, HBr, and HI on ice surface at 191 K in a fast-flow-tube reactor.[26] The results showed that the reaction probability of HONO on HI-treated ice surface is higher than that on HCl-treated or HBr-treated ice surface. The reaction probability increased with the surface coverage of HI, and the product INO rapidly converted to I_2 on the HI-treated ice surface. However, chemical or photochemical conversion kinetics and mechanisms of iodide alone in frozen solution are unknown and needed to be investigated.

In this study, we investigated the oxidation of iodide to form I_3^- and I_2 in frozen solution, which is even more enhanced under simulated solar irradiation. The effects of various experimental parameters on the freezing-enhanced iodide oxidation were systematically investigated to understand this anomalous chemical process. A modeling study was also carried out to reproduce the experimental results. This finding proposes a previously unrecognized source of gaseous I_2 through abiotic process in the polar region.

EXPERIMENTAL SECTION

Materials. KI (99.5%, Samchun Chemical) was used as the iodide source. N_2 (BOC Gases, 99.999% purity) and O_2 (Sinan Gases, Korea, 99.999% purity) gases were used when the effect of the dissolved gas was investigated. Ultrapure deionized water (18 MΩ·cm) prepared by a Barnstead purification system was used in all experiments.

Laboratory Experiments of Iodide Oxidation in Ice. The initial iodide concentration employed in this work ranged in 1−1000 μM for the oxidation either in the dark or under photo-irradiaion. The pH of the solutions was adjusted with HCl or NaOH solution to a desired value prior to freezing. Iodide solution (5 mL) was added to 12 × 125 mm quartz tubes, sealed with septa, and put into the ethanol bath, which was precooled at −5 °C. The temperature of the freezing bath was gradually lowered from −5 °C to −20 °C within 30 min for complete solidification. The whole ice column was irradiated by a lamp (for photo-oxidation) after the freezing process. Sample tubes (maximum 16 tubes) were located in a merry-go-round photolysis reactor that was rotated at a constant speed (0.8−1.0 rpm) around a 100 W mercury lamp (Ace Glass Inc.) for uniform irradiation. Light was filtered by a pyrex jacket (transmitting λ > 300 nm; see Figure 1C) surrounding the mercury lamp that was immersed in the ethanol bath. For the photo-oxidation experiments in oxygen or nitrogen saturated conditions, the sample tubes were purged with O_2 or N_2 gas for 30 min prior to freezing and irradiation. The dark oxidation experiments were also carried out in the same way except for the photoirradiation.

All irradiated ice samples were thawed for sampling and the subsequent analysis for I_3^-. Although there is a possibility that the concentration of tri-iodide in frozen solution might be changed after thawing, we assumed that this effect is negligible in this study. Aqueous photochemical reactions of iodide were also carried out as a control at 25 °C using the same experimental setup. The concentration of photogenerated tri-iodide (I_3^-) was determined by measuring the absorbance at 352 nm (ε_m = 26400 $M^{-1}cm^{-1}$)[23] using a UV−visible spectrophotometer (Libra S22). The detection limit of this analysis method is about 0.1 μM of tri-iodide. The absorption spectrum of oxygen-saturated solution of iodide was obtained with direct O_2 purging in a quartz cell (path length of 1 cm) sealed with septa.

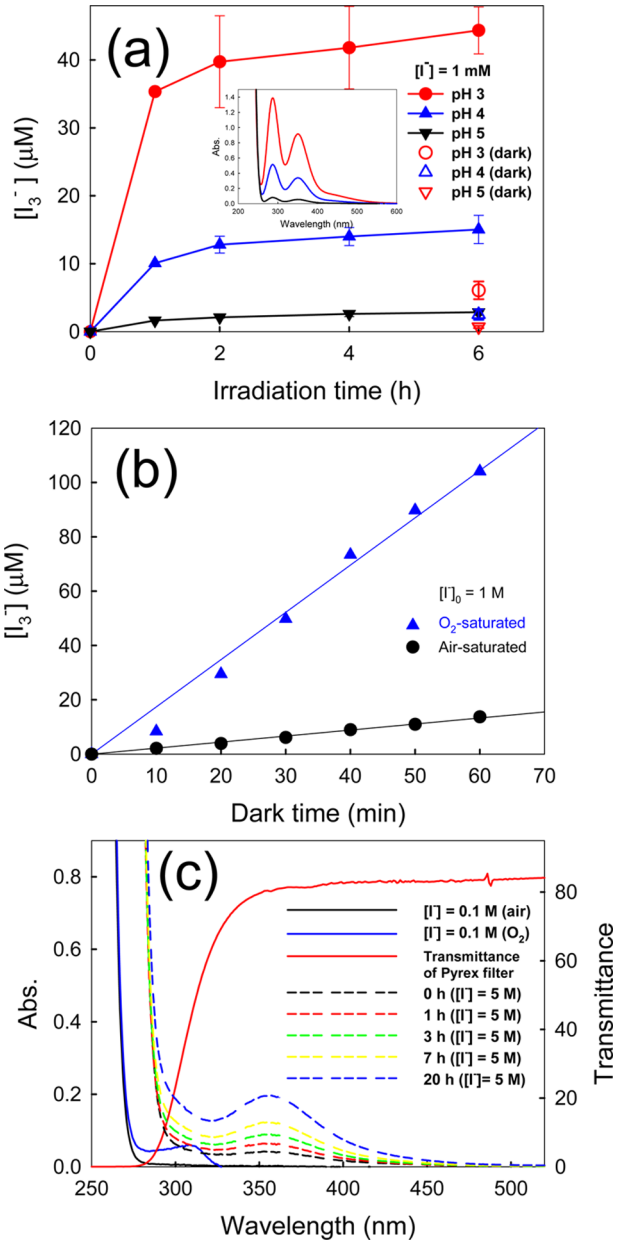

Figure 1. Iodide oxidation to I_3^- in frozen and aqueous solution. (a) The time profiles of the photogeneration of tri-iodide in the ice phase (−20 °C) measured at different pH along with the dark control oxidation of iodide shown. (Inset: UV−visible absorption spectra of I_3^- formed in ice containing $[I^-]_0$ = 1 mM, after 2 h of irradiation). (b) The time profiles of dark production of tri-iodide from a concentrated iodide solution that was continuously purged with pure O_2 or air flow ($[I^-]_0$ = 1 M, pH_i = 3). (c) UV−visible absorption spectra of iodide solutions. Dashed lines represent the spectral change of an iodide solution ($[I^-]_0$ = 5 M, pH_i = 6.5, air-equilibrated, dark condition) with time with the accompanying production of I_3^-. Note the appearance of ($I^-{\cdot}O_2$) charge-transfer (CT) complex band in O_2-saturated solution (blue solid line, $[I^-]_0$ = 0.1 M). The transmittance of the pyrex filter employed for photo-experiments was also shown (red solid line) for comparison.

DOI: 10.1021/acs.est.5b05148
Environ. Sci. Technol. 2016, 50, 1280−1287

Outdoor Experiments. The experiments for iodide photo-oxidation were also carried out under ambient solar radiation. The outdoor experiments were conducted in the Antarctic region, King George Island (62°13′S 58°47′W, sea level) from December 1 to 17, 2010. Quartz tubes containing the desired concentration of iodide were frozen in a refrigerator (at −20 °C) before exposing to sunlight. The solidified ice samples were placed on the surface of ambient snow horizontally for exposure to incident solar radiation. The irradiated samples remained solid during the entire exposure to sunlight. Control photolyses of aqueous samples containing iodide were carried out simultaneously under the same irradiation conditions. To prevent the freezing of the aqueous samples under ambient exposure, we placed the samples on an electrically heated mat on the snow.

The concentrations of photogenerated I_3^- were immediately determined by UV−visible spectrophotometer after solar irradiation in the Korea Polar Research Institute (KOPRI) King Sejong Station (King George Island). The ambient temperature ranged between −4.5 and 2.3 °C (average temperature was −3.5 °C during experiments). The integrated solar irradiance as measured at the King Sejong Station in King George Island varied from 0.2 to 8.6 W/m^2 for UV band of 315 < λ < 380 nm, depending on the angular position of the sun and the weather condition, with an average intensity of 3.1 W/m^2 during the photo-oxidation experiment (corresponding to about 9.0 (μeinstein m^{-2}s^{-1}) assuming 350 nm photons). The snow samples for iodide spiking experiment were collected 100 m far from The King Sejong Station and about 50 m far from sea ice and seawater. The initial pH of collected snow and glacier ice after melting was 5.30 and 5.45, respectively. The glacier ice samples were obtained from drifting icebergs detached from Marian Cove Glacier, and the outer part of glacier was removed to eliminate contamination. The collected snow and glacier were thawed at room temperature and resolidified after iodide spiking (adding 1 mM iodide) at −20 °C for photolysis under natural solar irradiation.

Gaseous I_2 Measurement by Cavity Ring-Down Spectroscopy. Gaseous iodine molecule was measured by cavity ring-down spectroscopy (CRDS). The principle of CRDS and pertinent experimental details (Figure S1) are described elsewhere,[27] and a brief description is given here. The photo-oxidation of iodide in frozen solution proceeded in a Pyrex glass cell (41 mm internal diameter and 54 cm length) coupled with two valves on both sides of the cell (total volume =770 ± 10 mL). The glass cell consists of a double pipe. To minimize possible secondary reactions, we washed the inner side of the cell with deionized water and methanol before each experiment and dried. Aqueous NaI solutions ([NaI] = 1, 5, 10, 50, and 100 μM, volume = 50 mL) were prepared by reagent grade NaI (Sigma-Aldrich, ≥ 99.5%) in 18 MΩ·cm deionized water. Deoxygenated water was also used for control experiments. Dissolved oxygen was removed from deionized water by bubbling nitrogen gas through the water, the concentration of which was measured with a dissolved oxygen meter. Typical concentrations of dissolved oxygen were 8.2−8.4 mg/L and 0.0−0.2 mg/L before and after nitrogen gas bubbling, respectively. Solution pH was adjusted to pH 3 by adding HCl. The temperature of the inner side of the cell was regulated by flowing a mixture of ethylene glycol and water through the outer side of a double pipe cell over the range of 253 to 298 K. The sample solution was filled into the cell at 265 K, and the temperature of the inner side of the cell was gradually decreased. It took about 40 min for the temperature of the ice sample to reach 253 K. The temperature of the sample ice was monitored by a thermocouple, which was located near the ice surface.

The sample ice (surface area of 145 cm^2) kept at 253 K was illuminated through a Pyrex glass cell by two 20 W fluorescence lamps (TOSHIBA, FL-20S-BLB, 58 cm length, centered at 365 nm) in a closed-batch reactor. Each lamp was fixed above the cell. The distance between the center of the lamp and the ice surface was 7.0(±0.2) cm, and the incident irradiation power was 8.25(±0.25) mW cm^{-2}, corresponding to about 1.5 × 10^{16} photons cm^{-2} s^{-1}. After irradiation for 3 h, the sample ice was thawed at 298 K. It took about 10 min for the temperature of the sample solution to reach 298 K, and then the molten solution was at rest for 15 min to achieve equilibrium. The CRDS detection region was 18.3(±1) mm above the surface of the sample solution. The I_2 concentration was monitored with a Nd^{3+}−YAG-pumped dye laser (Lambda Physik, SCANmate) at 532.8 nm for the $B^3\Pi-X^1\Sigma^+$ band. The CRDS measurements of gaseous I_2 were usually carried out after thawing the ice at 298 K. In a separate control experiment, I_2 was measured both before and after melting the ice to investigate whether gaseous I_2 is emitted over the frozen state at 253 K. The measurement was performed immediately after two valves on both sides of the reactor cell were opened, and no apparent sign of I_2 loss was observed during the measurement. The I_2 signal baseline was taken at the same wavelength after refreshing the cell completely by $N_2(g)$ flow. The detection limit of I_2 was estimated to be 1.5 × 10^{10} molecules cm^{-3}. All photochemical reactions and measurements were performed at atmospheric pressure. The pressure in the cell was monitored by a pressure gauge.

Modeling. We use the multiphase model, CON-AIR (condensed-phase-to-air transfer model).[28,29] The model treats the coupling of ice photochemistry (i.e., in the brine layer (BL)), and atmospheric boundary layer and condensed-phase chemistry. The model is composed of reactions involving O, H, C, N, S, Cl, Br, and I, incorporating heterogeneous uptake, halogen recycling on deliquesced airborne sea-salt aerosols, and wet−dry deposition. Full model details with a list of the condensed-phase reactions, phase-transfer processes, and photochemical reactions used in the model can be found elsewhere.[28,29] A list of BL reactions and the Henrýs law constants included in the model is included in Table S1 and S2. The dependence of the Henry's law constants on the salinity was not considered due to the lack of the experimental data. Halogen species exchange between the BL and gas phase is treated via phase equilibration as well onto the sea-ice surface. The solubility of species is taken into account by including a diurnal variation of the typical temperature profile during polar springtime (i.e., $\sim 260 \leq T/K \leq \sim 270$).[30] CON-AIR is parametrized with $[I^-]_0$ = 1.3 × 10^{-7} M; a BL thickness of 500 μm; volumetric =1.14 × 10^{-6} (cm^3 (BL)/cm^3 (atmosphere), $[O_2]$(sea ice) = 1 × 10^{-4} M,[31] which is applied to aqueous-phase reaction rates; and the first-order transfer rate constant, k_t = 1.25 × 10^{-5} s^{-1}[32,33] and the dimensionless Henry's law constant ($H' = HRT$, H is a species' Henry's law constant, R is the gas constant, 0.08206 L atm K^{-1} mol^{-1} and T is the temperature (K) are used to quantify the rate of transfer of species from the BL to the atmosphere via $k_{(BL\rightarrow atmosphere)} = (k_t \times [\text{species concentration}])/(H')$.[28,29] We have implemented in CON-AIR the experimentally derived reaction 1 (vide infra) and the equilibrium between tri-iodide and I_2. For a

DOI: 10.1021/acs.est.5b05148
Environ. Sci. Technol. 2016, 50, 1280−1287

Table 1. Production of I_3^- (μM) in Aqueous Solution and Ice

	Dark		Light						Antarctic Solar			
Phase	Aq	Ice	Aq			Ice			Aq (DW)‡	Ice (DW)	Snow	Glacier
Gas†	Air	Air	Air	O_2*	N_2*	Air	O_2*	N_2*	Air	Air	Air	Air
pH 3	*nd*	6.1±1.3	2.9	11.0±1.7	*nd*	44.3±3.5	47.3±1.2	0.3±0.1	4.0±0.1	29.4±1.5		
pH 4	*nd*	2.5±0.8	0.3±0.1	1.3±0.3	*nd*	15±2.1	19.9±0.2	0.2±0.1	0.8±0.2	13.2±1.2		
pH 5	*nd*	0.7±0.2	0.1	0.1	*nd*	2.9±0.5	2.6±0.3	*nd*	*nd*	1.8±0.1	1.5±0.1	0.4
pH 6	*nd*	0.1	*nd*	*nd*	*nd*	2.3	0.6±0.1	*nd*	*nd*	*nd*		

Experimental conditions: $[I^-]_0$ = 1 mM, 6 h of irradiation; snow and glacier samples were also spiked with 1 mM iodide. †Type of dissolved gas prior to freezing. *O_2 or N_2 was purged for 30 min before freezing and irradiation. ‡DW: distilled water. nd: not detected

detailed description of CON-AIR, please refer to the previous studies.[28,29] This allows us to study the effect of the proposed mechanism, under a range of aqueous iodide concentrations and pH values, on the release of active iodine to the atmosphere and the resulting contribution to iodine levels in the polar boundary layer.

RESULTS AND DISCUSSION

Iodide Oxidation to Tri-iodide in Various Conditions. Iodide can be oxidized to tri-iodide slowly in the presence of O_2 in acidic condition through reaction 1.[25,34]

$$O_2(aq) + 4H^+ + 6I^- \rightarrow 2H_2O + 2I_3^- \quad (1)$$

The rate constant of reaction 1 was first measured in ambient aqueous solution and determined to be 2.16×10^{-2} ($mol^{-2} \cdot L^2 \cdot s^{-1}$) (see Table S3 and Figure S2 for details). We found that the oxidative formation of tri-iodide (reaction 1), which occurs extremely slowly in aqueous solution, is significantly accelerated in the frozen solution (both under dark and photo-irradiation conditions) (see Figure 1a). The inset (Figure 1a) clearly shows the appearance of the tri-iodide peak, which has two absorption bands centered at 288 and 352 nm (with molar absorption coefficients of 40 000 and 26 400 $M^{-1}cm^{-1}$, respectively). To confirm the occurrence of reaction 1 even in the absence of light, we monitored the absorbance band (at 352 nm) as a function of time under dark condition in a highly concentrated iodide solution (1 M): Figure 1b shows that the tri-iodide absorbance gradually increased with time, which indicates that I_3^- is generated in situ as a result of the reaction between iodide and dissolved O_2. The oxygen purging of the iodide solution further accelerated the production of tri-iodide (Figure 1b), which confirms the role of O_2 in reaction 1. However, reaction 1 is negligible in aquatic environmental conditions, where the iodide concentration is much lower. Upon observing the enhancement of iodide oxidation in frozen solution, we systematically studied the iodide activation in ice medium as a new unknown environmental transformation path and investigated the oxidation of iodide to tri-iodide (I_3^-) in ice and the subsequent emission of gaseous I_2 to the gas phase.

Table 1 summarizes the production of I_3^- in aqueous solution and ice under different experimental conditions (i.e., in the presence and absence of light and O_2, various pH, and solar radiation in the polar environment): the formation of I_3^- in ice was significantly accelerated in all tested conditions compared to those in the liquid state. The production of tri-iodide was observed in ice even in the dark acidic condition, whereas that in aqueous solution was negligible below the detection limit. Under solar irradiation (λ > 300 nm), the rate of tri-iodide formation was significantly enhanced in ice, although iodide ions do not absorb light in this wavelength region (Figure 1c). Although the photogeneration of tri-iodide (under solar-simulating condition) gradually decreased from pH 3 to pH 6, the enhanced production of tri-iodide in the ice phase was still observed over a wide range of pH (3–9) (Figure 2). In the absence of light, the generation of tri-iodide in ice exhibited a similar pH dependence although the dark production rates were much lower than the photoproduction rates. The ice-induced production of I_3^- under dark was about seven times lower than that under light irradiation (at pH 3) and became insignificant above pH 6.

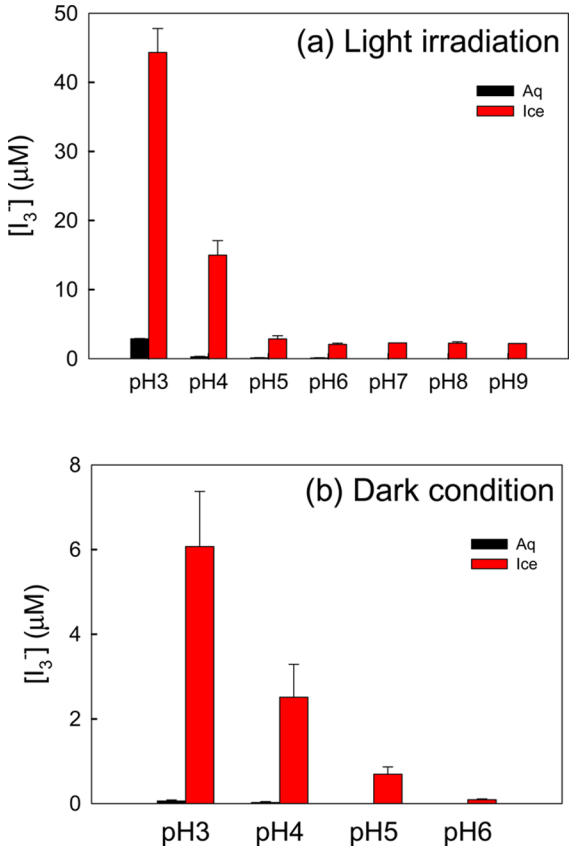

Figure 2. Generation of I_3^- at various pH range in aqueous solution at 25 °C (black bar) and in ice at −20 °C (red bar). (a) Under light irradiation (λ > 300 nm) and (b) in the dark; $[I^-]_0$ = 1 mM, reaction time 6 h.

The dissolved gas (air, N_2, and O_2) also critically influenced the photo-oxidation of iodide as shown in Table 1. Because the efficiency of iodine atom formation via photoexcitation of

DOI: 10.1021/acs.est.5b05148
Environ. Sci. Technol. 2016, 50, 1280−1287

iodide ion is highly enhanced in the presence of a suitable electron acceptor such as dioxygen,[35] the photo-oxidation of iodide was negligible in both aqueous and frozen solutions in the absence of O_2. The photogeneration of tri-iodide in aqueous solution was markedly enhanced in oxygen-saturated conditions in an acidic environment, which confirms the role of dioxygen in the photo-oxidation of iodide. However, it is noted that there was no significant change of tri-iodide formation between air-equilibrated and O_2-saturated conditions in the ice phase, which implies that O_2 is saturated in ice-grain boundaries even in air-saturated conditions. Previous studies also showed a similar result indicating that the dissolved O_2 can be accumulated in the ice-grain boundary upon freezing.[14,24]

The photo-oxidation of iodide was also investigated as a function of initial iodide concentration in ice phase at acidic pH range (Figure 3). The generation of tri-iodide in ice gradually

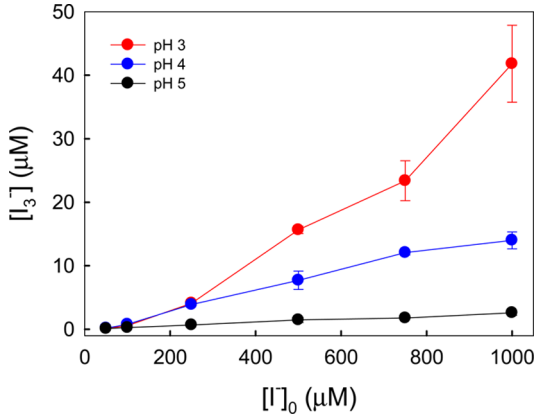

Figure 3. Photo-induced production of I_3^- from iodide oxidation in ice. The tri-iodide concentration generated after 6 h of solar-simulating irradiation in the ice phase (−20 °C) was measured as a function of the initial iodide concentration and pH.

increased with increasing initial concentration of iodide and was more efficient at lower pH condition in the whole concentration range tested. We also carried out the iodide photo-oxidation experiments at various temperature (−10, −20, and −30 °C), which are shown in Figure S3. A similar enhancement of iodide oxidation was observed at different freezing temperatures, and we did not observe any formation of KI precipitates during the experiments.

Mechanism for Enhanced Oxidation of Iodide in Ice. At lower pH and higher iodide concentrations, the generation of tri-iodide in ice is higher (Figures 2 and 3). The observed accelerated generation of tri-iodide in illuminated and dark ice conditions can be ascribed to the freeze concentration effect of iodide and O_2 (in reaction 1) at ice grain−surface boundaries. The local concentration of solutes in the ice-grain boundary region can be enhanced by several orders of magnitude from their respective aqueous concentrations.[36−38] Reaction 1 is negligible in diluted aqueous solutions but can be markedly accelerated in high concentrations found in the ice grain boundary region. Furthermore, the elevated local concentrations of substrates in the ice grain boundary region may affect the photochemical kinetics and mechanisms.[36,39] Our results show that the photogeneration of tri-iodide in ice was higher at lower pH (as shown in Figures 1a and 2a), because reaction 1 is favored under acidic condition.

Although iodide itself does not absorb in the wavelength region of $\lambda > 300$ nm (Figure 1c), it can form a charge-transfer (CT) complex with O_2 ($I^-{\cdot}O_2$).[40] The absorption spectrum of a concentrated iodide solution is different between the air-saturated and O_2-saturated condition (Figure 1c): a new absorption band at 280−330 nm appeared in an O_2-saturated solution (see Figure S4 for detailed spectrum), which agrees with the reported absorption spectrum of the CT complex ($I^-{\cdot}O_2$) in aqueous solution.[40] The CT complexation (enabling the light absorption above 300 nm) should be enhanced in the ice-grain boundary region, where both iodide and dioxygen can be concentrated, which subsequently accelerates the photoinduced oxidation of iodide (via reaction 2). In the presence of excess iodide in the grain boundary, an I atom recombines with I^- to produce I_2^- at a diffusion-limited rate, which subsequently generates tri-iodide through disproportionation (reactions 3 and 4).[41] In the confined environment of ice grain boundary, the bimolecular reactions among various reactive iodine species (I, I_2^-, I_3^-) and O_2 might be highly accelerated, which is associated with the marked photoeffect observed in iodide oxidation in ice.

$$I^- + O_2 \rightarrow (I^-{\cdot}O_2) \rightarrow I{\cdot} + O_2^- \quad (2)$$

$$I{\cdot} + I^- \rightarrow I_2^- \quad (3)$$

$$I_2^- + I_2^- \rightarrow I_3^- + I^- \quad (4)$$

Verification of Freeze Concentration Effect. To investigate the concentration effect of iodide and protons on the photo-oxidation kinetics of iodide, we monitored the formation of tri-iodide in the aqueous phase via elevating the concentration of either iodide or proton (lowering pH) (Figure 4). The generation of tri-iodide in aqueous solution was

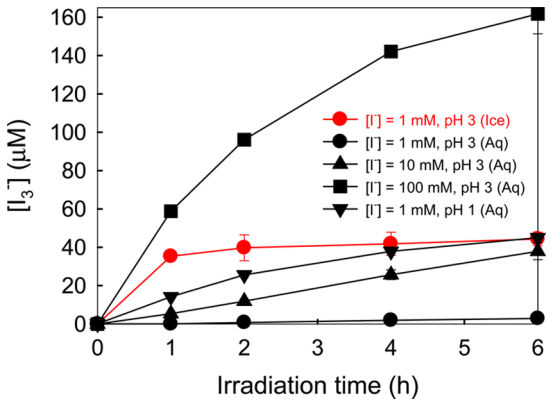

Figure 4. Effects of pH and iodide concentration on the photo-oxidation of iodide in aqueous solution and ice.

markedly enhanced when the iodide concentration is increased 100-fold (1 mM → 100 mM) or the proton concentration was increased 100-fold (pH 3 → pH 1). Hence, although the iodide photo-oxidation in aqueous solution at 1 mM and pH 3 is negligible, its kinetics in ice are significantly enhanced.

Direct Detection of Gaseous I_2 with CRDS. The production of tri-iodide implies the presence of I_2 that should be in equilibrium with tri-iodide ($I_2 + I^- \leftrightarrow I_3^-$: $K = 700$).[35,42] The I_2 molecule generated in ice can be released to the headspace. In laboratory experiments, the release of gaseous I_2 emitted from the irradiated frozen solution was directly detected by cavity ring-down spectroscopy (CRDS) (Figure

DOI: 10.1021/acs.est.5b05148
Environ. Sci. Technol. 2016, 50, 1280−1287

5a). The results show that the concentration of gaseous I_2 linearly increased with increasing iodide concentration (Figure 5b). The photogeneration of I_2 was observed in the irradiated frozen solution containing iodide as low as 1 μM (or about 0.1 ppm), which is close to a lower detection limit. The I_2 concentration produced at $[I^-] < 1$ μM could not be quantified.

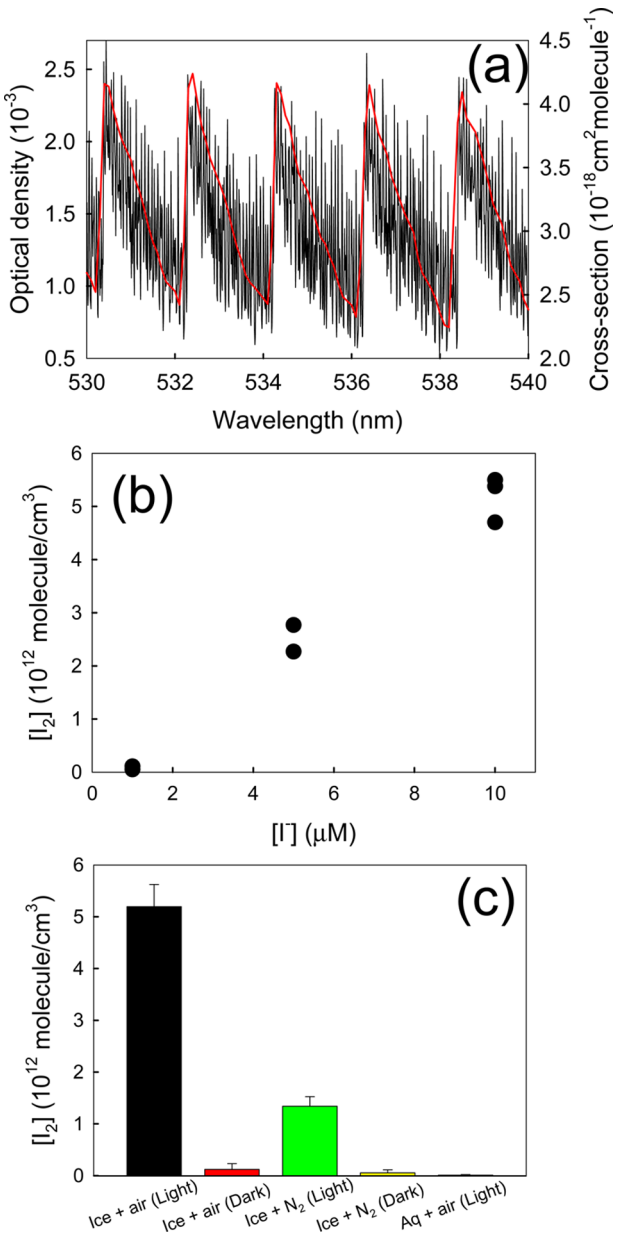

Figure 5. Detection of gaseous I_2 by CRDS. (a) CRD spectrum of gaseous I_2 formed as a result of iodide photo-oxidation in frozen NaI solution (10 μM, pH_i = 3) for 3 h at 253 K. The spectrum was measured after the frozen solution was thawed (at 298 K). (Red line) I_2 absorption cross-section reported in the literature.[48] (b) Concentration of gaseous I_2 emitted (after thawing) from the frozen iodide solution irradiated for 3 h at 253 K as a function of the iodide concentration before freezing. The 3σ detection limit of I_2 (σ: the standard deviation of the baseline noise) was estimated to be 1.5 × 10^{10} molecules cm^{-3}, which corresponded to the case of $[I^-]_0$ = 0.8 μM under the present experimental condition. (c) Comparison of I_2(g) concentrations under various experimental conditions (pH_i = 3, $[I^-]_0$ = 10 μM, ice temperature at 253 K, equilibrium temperature after thawing at 298 K).

The effects of O_2, photoirradiation, and freezing on the generation of gaseous I_2 are compared in Figure 5c, which reconfirms that the freezing process and the presence of O_2 are critical for the production of I_2. Although the in situ generated I_2 might react with other halide species such as chloride and bromide, it does not seem to be significant. Note that the photogeneration of I_2 (Figure 5c) was measured in the presence of excess amount of chloride (1 mM HCl, 100 fold higher than the iodide concentration). An additional control test in the presence of 1 mM Br^- (in the condition of Figure 5c) did not reduce the I_2 emission at all.

In a separate set of experiments, the concentration of gaseous I_2 was measured at the frozen state (irradiated for 3 h, $[I^-]_0$ = 10 μM) at 253 K, then clean N_2 gas purged the reactor to clear out I_2. It took about 10 min for the irradiated ice to thaw at 298 K under dark conditions. After the molten solution was equilibrated for 15 min, gaseous I_2 was measured again. The emission of gaseous I_2 was observed both before and after thawing the ice, which yielded the concentration of 3.8(±1.6) and 3.9(±1.2) (× 10^{12} molecules cm^{-3}), respectively. This observation implies that the gaseous I_2 can be emitted directly over the irradiated ice and snow containing iodide even without melting the frozen media, which can also explain IO observation in inner Antarctica, where no surface melt occurs.[43,44] Moreover, this also implies that the in-situ-generated I_2 can diffuse successfully through the ice-grain boundaries to the air above the ice surface.

Incidentally, the I_2 emission flux from the irradiated ice surface is roughly estimated as an example at specific experimental conditions (Figure 5c: pH_i = 3, $[I^-]_0$ = 10 μM, air-equilibrated ice at 253 K, assuming that the production rate of I_2 is linear during the 3 h irradiation): the calculated photogeneration flux of I_2 in the CRDS reactor is 2.8 × 10^9 molecules cm^{-2} s^{-1}. Although this number should not be taken as an index for a real polar I_2 emission flux (because the laboratory experimental condition has much higher $[I^-]$ and UV flux and lower pH than those of the natural polar condition), it may provide an upper limit. However, the flux of I_2 emission via the dark aqueous reaction at 298 K (reaction 1) can be estimated on the basis of the experimentally determined rate law (see Table S3 and Figure S2) and the assumption that the production rate of I_2 is equal to that of I_3^- and all I_2 molecules are fully volatilized to the gas phase. The calculated I_2 flux under the dark aqueous condition in the same CRDS reactor would be 6.3 × 10^6 molecules cm^{-2} s^{-1}, which is lower by 3 orders of magnitude than the above-mentioned photogenerated flux of I_2.

Outdoor Experiments. Finally, the photo-oxidation of iodide (spiked into the molten snow and glacier samples) was investigated in the Antarctic region (King George Island, 62°13′N, 58°47′E) to confirm the laboratory-observed phenomenon under Antarctic solar radiation. The field experiments were carried out using the frozen solutions of iodide (in distilled water) and the refrozen solutions of molten snow and glacier (spiked with iodide), both of which were irradiated under the same Antarctic solar condition (Table 1). The outdoor experiments confirmed the laboratory results. The frozen samples irradiated under the Antarctic sun generated a significant amount of tri-iodide and I_2 (also confirmed by the appearance of the brownish color), which was more efficient at lower pH and higher iodide concentration.

Multiphase Modeling. We next incorporated the experimentally derived rate constant of reaction 1 into a multiphase

DOI: 10.1021/acs.est.5b05148
Environ. Sci. Technol. 2016, 50, 1280−1287

model[28,29] that considered the iodide oxidation and the reactions among active halogen species within the ice-grain boundary and its associated air-condensed phase equilibrium to calculate the effect of the proposed mechanism upon the gas-phase levels of iodine in the polar atmosphere. Competition between chloride, bromide, and iodide is quantitatively expressed in CON-AIR.[28,29] To show that the model replicates the laboratory experimental data, we conducted a modeling exercise to reproduce the range of I_2 production in the CRDS reactor condition ($[I^-]_0$ = 1 to 10 μM), which indeed exhibits a good match (with Figure 5b) as shown in Figure S5.

The model results indicate that the photo-oxidation of iodide in ice, and the subsequent phase equilibration of I_2, produces the following gas phase IO levels under typical springtime Antarctic irradiation conditions: 0.25 pptv and 1.5 pptv with $[I^-]_0$ = 10 nM at pH 6 and 3, respectively; 0.5 pptv and 2.5 pptv with $[I^-]_0$ = 130 nM for pH 6 and 3, respectively. These model results were obtained with a modeling framework based on available experimentally- and field-derived data; however, please note that uncertainties still remain when modeling processes at the ice−air interface; for instance, on the concentration effects applied to reaction rates, salinity dependence of Henry's law coefficients, and brine-layer thickness. This range of IO concentrations are in agreement with satellite observations around King George Island.[45] The modeled IO dependence on pH reflects the enhanced production of tri-iodide at acidic condition, as observed in the laboratory experiments. The pH of the sea-ice and snowpack at Antarctica ranges in 4.5−6.5.[46] Our results suggest that higher levels of reactive iodine are expected to be transferred to the gas phase in regions with higher iodide concentrations. However, we should mention that the total I_2 emission from the solar-irradiated ice surface in the polar environment is not comparable (on a global scale) to the total iodine emission from seawater, considering that the sea surface area is far larger than the frozen surface on earth.

Environmental Implications. We have shown that the abiotic oxidation mechanism of iodide to tri-iodide and I_2 in the ice phase, under solar irradiation, leads to the emission of gaseous reactive iodine. The experimental studies were carried out with varying the reaction conditions (e.g., pH, light intensity, iodide concentration, and dissolved gas), and the observed phenomenon may have significant environmental implications because iodine compounds can influence the chemistry and radiative balance of the polar atmosphere. The modeling calculation done with employing the environmentally relevant condition confirmed that the proposed iodide oxidation process can be important in the polar environment. Furthermore, the strong enrichment of iodine in Antarctic meteorites and snow, which has recently been measured,[11,47] might be related with the enhanced production of volatile I_2 and IO over the solar-irradiated ice. Freezing-induced chemical reactions involving iodine compounds, which have not been recognized before, may have significant impacts on polar environments. This kind of phenomenon might be extended to other halide species concentrated in brine channels in sea ice and should be further investigated.

■ ASSOCIATED CONTENT

Supporting Information

The Supporting Information is available free of charge on the ACS Publications website at DOI: 10.1021/acs.est.5b05148.

Figures showing a schematic diagram of the experimental setup of a photochemical reactor cell coupled with CRDS; kinetic experiments for the rate constant determination for the reaction 1; temperature effect on iodide photo-oxidation; UV−visible absorption spectrum of CT complex ($I^-\cdot O_2$); and model simulations of the experimental results. Tables showing QLL reactions and rate constants and Henry constants of iodine species. (PDF)

■ AUTHOR INFORMATION

Corresponding Author

*Tel: +82-54-279-2283; fax: +82-54-279-8299; e-mail: wchoi@postech.edu

Notes

The authors declare no competing financial interest.

■ ACKNOWLEDGMENTS

Funding for this work was provided by Korea Polar Research Institute (KOPRI) project (PP16010), the KOPRI "Polar Academic Program (PAP)", grants-in-aid from JSPS (Grants No. 23651014 and 23684045) and the Kurata Memorial Hitachi Science and Technology Foundation. We thank Ibrahim Diallo from Medgar Evers College aiding the literature information translation.

■ REFERENCES

(1) von Glasow, R. Sun, sea and ozone destruction. *Nature* **2008**, *453* (7199), 1195−1196.

(2) Pratt, K. A.; Custard, K. D.; Shepson, P. B.; Douglas, T. A.; Pöhler, D.; General, S.; Zielcke, J.; Simpson, W. R.; Platt, U.; Tanner, D. J.; Gregory Huey, L.; Carlsen, M.; Stirm, B. H. Photochemical production of molecular bromine in Arctic surface snowpacks. *Nat. Geosci.* **2013**, *6* (5), 351−356.

(3) Saiz-Lopez, A.; von Glasow, R. Reactive halogen chemistry in the troposphere. *Chem. Soc. Rev.* **2012**, *41* (19), 6448−6472.

(4) Abbatt, J. P. D.; Thomas, J. L.; Abrahamsson, K.; Boxe, C.; Granfors, A.; Jones, A. E.; King, M. D.; Saiz-Lopez, A.; Shepson, P. B.; Sodeau, J.; Toohey, D. W.; Toubin, C.; von Glasow, R.; Wren, S. N.; Yang, X. Halogen activation via interactions with environmental ice and snow in the polar lower troposphere and other regions. *Atmos. Chem. Phys.* **2012**, *12* (14), 6237−6271.

(5) Saiz-Lopez, A.; Plane, J. M. C.; Baker, A. R.; Carpenter, L. J.; von Glasow, R.; Gómez Martín, J. C.; McFiggans, G.; Saunders, R. W. Atmospheric chemistry of iodine. *Chem. Rev.* **2012**, *112* (3), 1773−1804.

(6) Saiz-Lopez, A.; Plane, J. M. C.; Mahajan, A. S.; Anderson, P. S.; Bauguitte, S. J. -B.; Jones, A. E.; Roscoe, H. K.; Salmon, R. A.; Bloss, W. J.; Lee, J. D.; Heard, D. E. On the vertical distribution of boundary layer halogens over coastal Antarctica: implications for O_3, HOx, NOx and the Hg lifetime. *Atmos. Chem. Phys.* **2008**, *8* (4), 887−900.

(7) Schroeder, W. H.; Anlauf, K. G.; Barrie, L. A.; Lu, J. Y.; Steffen, A.; Schneeberger, D. R.; Berg, T. Arctic springtime depletion of mercury. *Nature* **1998**, *394* (6691), 331−332.

(8) Simpson, W. R.; Brown, S. S.; Saiz-Lopez, A.; Thornton, J. A.; von Glasow, R. Tropospheric Halogen Chemistry: Sources, Cycling, and Impacts. *Chem. Rev.* **2015**, *115* (10), 4035−4062.

(9) Simpson, W. R.; von Glasow, R.; Riedel, K.; Anderson, P.; Ariya, P.; Bottenheim, J.; Burrows, J.; Carpenter, L. J.; Frieß, U.; Goodsite, M. E.; Heard, D.; Hutterli, M.; Jacobi, H.-W.; Kaleschke, L.; Neff, B.; Plane, J.; Platt, U.; Richter, A.; Roscoe, H.; Sander, R.; Shepson, P.; Sodeau, J.; Steffen, A.; Wagner, T.; Wolff, E. Halogens and their role in polar boundary-layer ozone depletion. *Atmos. Chem. Phys.* **2007**, *7* (16), 4375−4418.

DOI: 10.1021/acs.est.5b05148
Environ. Sci. Technol. 2016, 50, 1280−1287

(10) Saiz-Lopez, A.; Mahajan, A. S.; Salmon, R. A.; Bauguitte, S. J. -B.; Jones, A. E.; Roscoe, H. K.; Plane, J. M. C. Boundary layer halogens in coastal antarctica. *Science* **2007**, *317* (5836), 348−351.
(11) Frieß, U.; Deutschmann, T.; Gilfedder, B. S.; Weller, R.; Platt, U. Iodine monoxide in the Antarctic snowpack. *Atmos. Chem. Phys.* **2010**, *10* (5), 2439−2456.
(12) Betterton, E. A.; Anderson, D. J. Autoxidation of N(III), S(IV), and other species in frozen solution − A possible pathway for enhanced chemical transformation in freezing systems. *J. Atmos. Chem.* **2001**, *40* (2), 171−189.
(13) Grannas, A. M.; Jones, A. E.; Dibb, J.; Ammann, M.; Anastasio, C.; Beine, H. J.; Bergin, M.; Bottenheim, J.; Boxe, C. S.; Carver, G.; Chen, G.; Crawford, J. H.; Dominé, F.; Frey, M. M.; Guzmán, M. I.; Heard, D. E.; Helmig, D.; Hoffmann, M. R.; Honrath, R. E.; Huey, L. G.; Hutterli, M.; Jacobi, H. W.; Klán, P.; Lefer, B.; McConnell, J.; Plane, J.; Sander, R.; Savarino, J.; Shepson, P. B.; Simpson, W. R.; Sodeau, J. R.; von Glasow, R.; Weller, R.; Wolff, E. W.; Zhu, T. An overview of snow photochemistry: evidence, mechanisms and impacts. *Atmos. Chem. Phys.* **2007**, *7* (16), 4329−4373.
(14) Takenaka, N.; Ueda, A.; Maeda, Y. Acceleration of the rate of nitrite oxidation by freezing in aqueous solution. *Nature* **1992**, *358* (6389), 736−738.
(15) Klanova, J.; Klan, P.; Nosek, J.; Holoubek, I. Environmental ice photochemistry: monochlorophenols. *Environ. Sci. Technol.* **2003**, *37* (8), 1568−1574.
(16) Cheng, J.; Soetjipto, C.; Hoffmann, M. R.; Colussi, A. J. Confocal fluorescence microscopy of the morphology and composition of interstitial fluids in freezing electrolyte solutions. *J. Phys. Chem. Lett.* **2010**, *1* (1), 374−378.
(17) Kim, K.; Choi, W.; Hoffmann, M. R.; Yoon, H.-I.; Park, B.-K. Photoreductive dissolution of iron oxides trapped in ice and its environmental implications. *Environ. Sci. Technol.* **2010**, *44* (11), 4142−4148.
(18) Kim, K.; Choi, W. Enhanced redox conversion of chromate and arsenite in ice. *Environ. Sci. Technol.* **2011**, *45* (6), 2202−2208.
(19) Jeong, D.; Kim, K.; Choi, W. Accelerated dissolution of iron oxides in ice. *Atmos. Chem. Phys.* **2012**, *12* (22), 11125−11133.
(20) Kim, K.; Yoon, H.-I.; Choi, W. Enhanced dissolution of manganese oxide in ice compared to aqueous phase under illuminated and dark conditions. *Environ. Sci. Technol.* **2012**, *46* (24), 13160−13166.
(21) Mock, T.; Thomas, D. N. Psychrophiles: from Biodiversity to Biotechnology. In *Microalgae in Polar Regions: Linking Functional Genomics and Physiology with Environmental Conditions*; Margesin, R., Schinner, F., Marx, J. C., Gerday, C., Eds.; Springer: Heidelberg, Germany, 2008; pp 285−308.
(22) Atkinson, H. M.; Hughes, C.; Shaw, M. J.; Roscoe, H. K.; Carpenter, L. J.; Liss, P. S. Halocarbons associated with Arctic sea ice. *Deep Sea Res., Part I* **2014**, *92*, 162−175.
(23) O'Driscoll, P.; Minogue, N.; Takenaka, N.; Sodeau, J. Release of nitric oxide and iodine to the atmosphere from the freezing of sea-salt aerosol components. *J. Phys. Chem. A* **2008**, *112* (8), 1677−1682.
(24) Takenaka, N.; Ueda, A.; Daimon, T.; Bandow, H.; Dohmaru, T.; Maeda, Y. Acceleration mechanism of chemical reaction by freezing: the reaction of nitrous acid with dissolved oxygen. *J. Phys. Chem.* **1996**, *100* (32), 13874−13884.
(25) O'Sullivan, D.; Sodeau, J. R. Freeze-induced reactions: formation of iodine-bromine interhalogen species from aqueous halide ion solutions. *J. Phys. Chem. A* **2010**, *114* (46), 12208−12215.
(26) Diao, G.; Chu, L. T. Heterogeneous reactions of HX + HONO and I_2 on ice surfaces: Kinetics and linear correlations. *J. Phys. Chem. A* **2005**, *109* (7), 1364−1373.
(27) Sakamoto, Y.; Yabushita, A.; Kawasaki, M.; Enami, S. Direct emission of I_2 molecule and IO radical from the heterogeneous reactions of gaseous ozone with aqueous potassium iodide solution. *J. Phys. Chem. A* **2009**, *113* (27), 7707−7713.
(28) Saiz-Lopez, A.; Blaszczak-Boxe, C. S.; Carpenter, L. J. A mechanism for biologically-induced iodine emissions from sea-ice. *Atmos. Chem. Phys.* **2015**, *15* (17), 9731−9746.
(29) Boxe, C. S.; Saiz-Lopez, A. Multiphase modeling of nitrate photochemistry in the quasi-liquid layer (QLL): implications for NO(x) release from the Arctic and coastal Antarctic snowpack. *Atmos. Chem. Phys.* **2008**, *8* (16), 4855−4864.
(30) Launiainen, J., Vihma, T. On the surface heat fluxes in the Weddell Sea. In *The Polar Oceans and Their Role in Shaping the Global Environment*; Johannessen, O. M., Muench, R. D., Overland, J. E.; Geophys. Monogr. Ser., Vol. *85*, Eds.; AGU: Washington, D.C., 2013; pp 399−419.
(31) Zhou, J.; Delille, B.; Brabant, F.; Tison, J.-L. Insights into oxygen transport and net community production in sea ice from oxygen, nitrogen and argon concentrations. *Biogeosciences* **2014**, *11* (23), 5007−5020.
(32) Gong, S. L.; Barrie, L. A.; Blanchet, J. P. Modeling sea-salt aerosols in the atmosphere 1. Model development. *J. Geophys. Res.* **1997**, *102* (3), 3805−3818.
(33) Michalowski, B. A.; Francisco, J. S.; Li, S.-M.; Barrie, L. A.; Bottenheim, J. W.; Shepson, P. B. A computer model study of multiphase chemistry in the Arctic boundary layer during polar sunrise. *J. Geophys. Res.* **2000**, *105* (D12), 15131−15145.
(34) Couto, A. B.; De Souza, D. C.; Sartori, E. R.; Jacob, P.; Klockow, D.; Neves, E. A. The catalytic cycle of oxidation of iodide ion in the oxygen/nitrous acid/nitric oxide system and its potential for analytical applications. *Anal. Lett.* **2006**, *39* (15), 2763−2774.
(35) Yeo, J.; Choi, W. Iodide-mediated photooxidation of arsenite under 254 nm irradiation. *Environ. Sci. Technol.* **2009**, *43* (10), 3784−3788.
(36) Heger, D.; Klanova, J.; Klan, P. Enhanced protonation of cresol red in acidic aqueous solutions caused by freezing. *J. Phys. Chem. B* **2006**, *110* (3), 1277−1287.
(37) Robinson, C.; Boxe, C. S.; Guzman, M. I.; Colussi, A. J.; Hoffmann, M. R. Acidity of frozen electrolyte solutions. *J. Phys. Chem. B* **2006**, *110* (15), 7613−7616.
(38) Heger, D.; Jirkovsky, J.; Klan, P. Aggregation of methylene blue in frozen aqueous solutions studied by absorption spectroscopy. *J. Phys. Chem. A* **2005**, *109* (30), 6702−6709.
(39) Kahan, T. F.; Donaldson, D. J. Benzene photolysis on ice: implications for the fate of organic contaminants in the winter. *Environ. Sci. Technol.* **2010**, *44* (10), 3819−3824.
(40) Levanon, H.; Navon, G. The spectrum and stability of oxygen iodide charge-transfer complex. *J. Phys. Chem.* **1969**, *73*, 1861−1868.
(41) Gardner, J. M.; Abrahamsson, M.; Farnum, B. H.; Meyer, G. J. Visible light generation of iodine atoms and I−I Bonds: Sensitized I^- oxidation and I_3^- photodissociation. *J. Am. Chem. Soc.* **2009**, *131* (44), 16206−16214.
(42) Rahn, R. O. Potassium iodide as a chemical actinometer for 254 nm radiation:use of iodate as an electron scavenger. *Photochem. Photobiol.* **1997**, *66* (4), 450−455.
(43) Atkinson, H. M.; Huang, R.-J.; Chance, R.; Roscoe, H. K.; Hughes, C.; Davison, B.; Schönhardt, A.; Mahajan, A. S.; Saiz-Lopez, A.; Hoffmann, T.; Liss, P. S. Iodine emissions from the sea ice of the Weddell Sea. *Atmos. Chem. Phys.* **2012**, *12* (22), 11229−11244.
(44) Schönhardt, A.; Richter, A.; Wittrock, F.; Kirk, H.; Oetjen, H.; Roscoe, H. K.; Burrows, J. P. Observations of iodine monoxide columns from satellite. *Atmos. Chem. Phys.* **2008**, *8* (3), 637−653.
(45) Schönhardt, A.; Begoin, M.; Richter, A.; Wittrock, F.; Kaleschke, L.; Gómez Martín, J. C.; Burrows, J. P. Simultaneous satellite observations of IO and BrO over Antarctica. *Atmos. Chem. Phys.* **2012**, *12* (14), 6565−6580.
(46) Ali, K.; Sonbawane, S.; Chate, D. M.; Siingh, D.; Rao, P. S. P; Safai, P. D.; Budhavant, K. B. Chemistry of snow and lake water in Antarctic region. *J. Earth Syst. Sci.* **2010**, *119* (6), 753−762.
(47) Heumann, K. G.; Gall, M.; H, W. Geochemical investigations to explain iodine-overabundances in Antarctic meteorites. *Geochim. Cosmochim. Acta* **1987**, *51* (9), 2541−2547.
(48) Saiz-Lopez, A.; Saunders, R. W.; Joseph, D. M.; Ashworth, S. H.; Plane, J. M. C. Absolute absorption cross-section and photolysis rate of I_2. *Atmos. Chem. Phys.* **2004**, *4* (5), 1443−1450.

DOI: 10.1021/acs.est.5b05148
Environ. Sci. Technol. 2016, 50, 1280−1287